

# Experiments on two-dimensional vortex patterns

D. Durkin and J. Fajans

*Department of Physics, University of California–Berkeley, Berkeley, California 94720-7300*

(Received 21 May 1999; accepted 18 October 1999)

The evolution of a strongly magnetized electron system is identical to that of an ideal two-dimensional (2-D) fluid; an electron column is equivalent to a fluid vortex. We have studied the stability of 2-D vortex patterns with electron columns confined in a Malmberg–Penning trap. The following cases are presented: the stability of  $N$  vortices arranged in a ring; the stability of  $N$  vortices arranged in a ring with a central vortex; the stability of more complicated vortex patterns.

© 2000 American Institute of Physics. [S1070-6631(00)00902-8]

## I. INTRODUCTION

In the late 1800s, the stability of two-dimensional (2-D) vortex patterns attracted attention because of its connection with a vortex model of the atom. Lord Kelvin solved the case of three vortices arranged in a ring,<sup>1</sup> but it was not until J. J. Thomson's Adams Prize essay of 1883 that the cases of three through seven vortices were solved, with instability predicted for seven vortices.<sup>2</sup> In 1931, T. H. Havelock generalized the calculation to  $N$  vortices arranged in a ring with a circular outer boundary, showing that  $N \geq 7$  was unstable.<sup>3</sup> He also considered the case of  $N$  vortices arranged in a ring with a fixed central vortex and demonstrated that a sufficiently strong central vortex could stabilize an otherwise unstable ring.

Experimentally, stable vortex patterns were first observed in rotating superfluid <sup>4</sup>He by Yarmchuk, Gordon, and Packard in 1979.<sup>4,5</sup> Vortices cooled into stable patterns as the superfluid interacted with the normal fluid component. As the experimenters had little control over the initial pattern, they could not test the stability of patterns directly. This experiment motivated Campbell and Ziff to computationally generate a catalog of stable 2-D vortex patterns for  $N = 1-30$  and for certain  $N$  up to 217, hereafter referred to as The Catalog.<sup>6,7</sup>

Stable vortex patterns have also been observed with electron columns confined in Malmberg–Penning traps. A Malmberg–Penning trap uses static magnetic and electric fields to confine electrons.<sup>8,9</sup> A simple trap, diagrammed in Fig. 1, consists of three coaxial, conducting cylinders contained within a high vacuum chamber. Radial confinement is provided by an axial magnetic field, about which the electrons gyrate. Axial confinement is provided by negatively biasing the end cylinders with respect to the central one, in which the electrons bounce back and forth. The electrons are destructively imaged by grounding one end cylinder, allowing them to stream along the magnetic field and onto a phosphor screen, producing a light image. This image is then detected by a charge-coupled device camera.

Under certain experimental conditions, the motion of a strongly magnetized electron column is bounce averaged along the magnetic field and the column behaves two dimensionally. A system of columns evolves by the interaction

with its self-electric field and is described by the 2-D Drift-Poisson equations, where  $\hat{\mathbf{z}}$  is along the magnetic field,  $\mathbf{v}(r, \theta, t)$  is the velocity,  $\phi(r, \theta, t)$  is the electrostatic potential, and  $n(r, \theta, t)$  is the  $z$ -averaged electron density.

$\mathbf{E} \times \mathbf{B}$  drift velocity:

$$\mathbf{v} = -\frac{1}{B} \nabla \phi \times \hat{\mathbf{z}}.$$

Poisson equation:

$$\nabla^2 \phi = \frac{e}{\epsilon_0} n.$$

Continuity equation:

$$\frac{\partial n}{\partial t} + \mathbf{v} \cdot \nabla n = 0.$$

Boundary condition:

$$\phi(r_{\text{wall}}, \theta, t) = 0.$$

These equations are identical to the 2-D Euler equations describing an ideal 2-D fluid; thus, the two systems evolve identically. The vorticity of the electron “fluid” is proportional to the electron density:

$$\boldsymbol{\Omega} \equiv \nabla \times \mathbf{v} = \frac{e}{\epsilon_0 B} n \hat{\mathbf{z}}.$$

Hence, a strongly magnetized electron column is equivalent to a 2-D fluid vortex.<sup>10-12</sup> Because we only trap electrons, we only have one sign of vorticity.

The formation of stable 2-D patterns in a Malmberg–Penning trap was first reported by Fine, Cass, Flynn, and Driscoll.<sup>13</sup> Their electron source was a spiral tungsten filament, which injected a spiral electron distribution. This distribution was Kelvin-Helmholtz unstable and produced many vortices (on the order of 100), which subsequently merged or were sheared away. They discovered that the decay of their system was sometimes arrested by the formation of stable patterns. This “crystallization” requires a cooling mechanism, which is not obvious in these electron systems, but could be due to interactions with background electrons,<sup>14,15</sup>

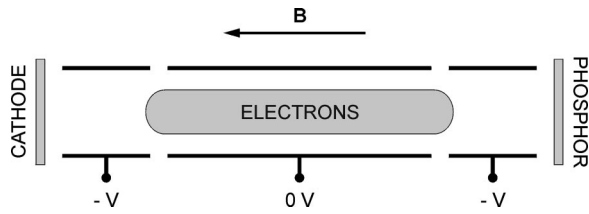


FIG. 1. The geometry of a simple Malmberg–Penning trap.

collisions with the background gas, or finite length effects. Note that they also had little control over the initial pattern.

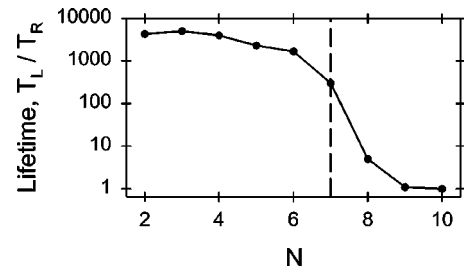
We constructed a Malmberg–Penning trap with a cesium antimonide photocathode as the electron source.<sup>16,17</sup> The photocathode provides increased control over the initial electron distribution, enabling us to inject arbitrary 2-D vortex patterns directly.

## II. EXPERIMENTAL PROCEDURE

To study the stability of a particular 2-D vortex pattern, we make a slide of the pattern using a printer with transparency film. The slide is illuminated with white light and projected onto the photocathode. Electrons are emitted only where there is light, so the initial electron pattern corresponds to the light image. The electron pattern is trapped, the hold time is varied, and the time for one bulk rotation ( $T_R$ ) and the pattern's lifetime ( $T_L$ ) are measured. Any new stable patterns that emerge from the dynamics are noted; this recrystallization into a new pattern may depend on the background electron density (see Sec. I), either injected initially or generated by the columns' dissipation.

A pattern is considered stable if  $T_L > 100 T_R$ , a time sufficient for point vortex dynamics, but before dissipative effects become significant.  $T_R$  is on the order of 1 ms, but depends on the pattern. The columns are observed to expand and dissipate on the order of 1 s. The electron–electron and electron–neutral collision times are on the order of 1 and 10 ms, respectively. Other possible dissipative mechanisms are finite temperature effects,<sup>18</sup> ‘rotational pumping,’<sup>19</sup> asymmetry-induced transport,<sup>20</sup> and long-range  $\mathbf{E} \times \mathbf{B}$  drift interactions.<sup>21</sup>

The radius of the individual electron columns is 0.050 cm, except where noted, to simulate the point vortex theories under study (it was not our goal to test patterns of finite size vortices,<sup>22</sup> though these experiments could be easily performed). The length of the columns is approximately that of the confinement region, 20 cm. The strengths of the individual columns are within 10% of the targeted values, as measured by the phosphor screen diagnostic. The patterns have an outer radius of 0.50 cm, corresponding to a radius normalized by the outer boundary radius (2.0 cm) of 0.25, except where noted. This radius is below the radii predicted to be unstable due to the effect of the boundary<sup>3</sup> (nonuniform photoemission in the outer regions of the photocathode prevented us from probing this stability criteria, but this experiment has been performed for the case of two vortices by Mitchell and Driscoll using electron columns<sup>23</sup>). The injected background electron density is more than a factor of 40 below the column density.

FIG. 2. Lifetime vs  $N$ , for  $N$  vortices arranged in a ring. The predicted  $N = 7$  stability limit is indicated by the dashed line.

We used a large magnetic field, 3 T, and a fast inject, 5  $\mu$ s, to reduce the smearing that occurs during a pattern's injection. The photocathode voltage is approximately  $-5$  V and the confinement gate voltages are  $-20$  V, close to the cathode voltage, to confine the longest possible electron columns and thereby reduce finite length blurring effects.<sup>18</sup> These parameters typically inject electron columns with a density of  $1 \times 10^7$   $\text{cm}^{-3}$  and a temperature of 1 eV, corresponding to a Debye length of 0.20 cm.

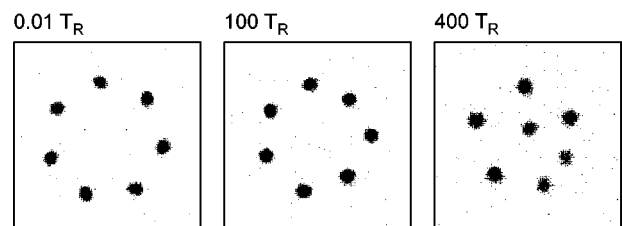
## III. $N$ VORTICES ARRANGED IN A RING

The problem of  $N$  vortices arranged in a ring was solved by Havelock. The experimental lifetimes for  $N=2-10$  are presented in Fig. 2 and demonstrate excellent agreement with his theory.

(1)  $N < 7$ : These patterns are stable ( $T_L > 1000 T_R$ ), as predicted.

(2)  $N = 7$ : This pattern is stable ( $T_L = 300 T_R$ ). Theoretically,  $N = 7$  patterns are neutrally stable with no boundary, but unstable with one. We have a boundary, but the normalized ring radius is 0.25 and therefore the influence of the boundary should be small. Sometime after  $300 T_R$ , the ring evolves into a new stable pattern with six vortices in a ring with one central vortex (the only stable  $N = 7$  pattern in The Catalog, see Fig. 3). This recrystallization occurs very late in the pattern's evolution and could be facilitated by the background electron density generated by the columns' dissipation.

(3)  $N > 7$ : These patterns are unstable ( $T_L \approx 1 T_R$ ), as predicted. The  $N = 8$  ring evolves into seven vortices in a ring with one central vortex (the only stable  $N = 8$  pattern in The Catalog). The  $N = 9$  ring evolves into eight vortices in a ring with one central vortex (the most stable  $N = 9$  pattern in The Catalog). The recrystallization of the  $N = 8$  and 9 patterns could be facilitated by the injected background electron

FIG. 3. The  $N = 7$  evolution. A new stable pattern emerges at  $400 T_R$  and lives for another  $1000 T_R$ .

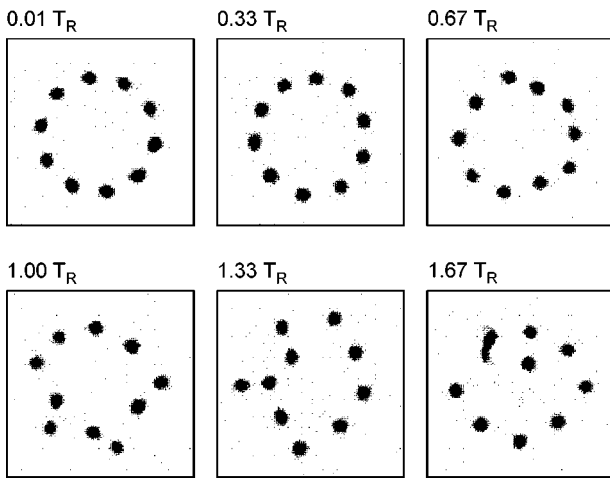


FIG. 4. The  $N=10$  evolution. Two vortices merge at  $1.67 T_R$  and no stable pattern emerges.

density, since these patterns emerge very early during the pattern's evolution ( $\approx 10 T_R$ ). The  $N=10$  ring rearranges and two vortices merge at  $1.67 T_R$  (Fig. 4); no stable pattern evolves.

#### IV. $N$ VORTICES ARRANGED IN A RING WITH A CENTRAL VORTEX

The problem of  $N$  vortices arranged in a ring with a fixed central vortex was also solved by Havelock. Physically, a fixed central vortex could be simulated by a wire along the trap's axis. In our experiments, though, the central vortex is free to move, and this case has been considered by a number of authors, including Morikawa and Swenson<sup>24</sup> and Campbell.<sup>25</sup> Freeing the central vortex allows it to go unstable and introduces an upper stability limit on the central vortex's strength. The lower limit corresponds to the ring vortices going unstable, as in Sec. III.

Recently, Lansky and O'Neil have analyzed the effect of a circular outer boundary on the central vortex's stability limits.<sup>26</sup> In our experiments, the ring's small normalized radius affects the stability limits by less than 1%, below the accuracy to which we can control a column's density and radius.

The strength of an electron column is given by  $\Gamma = n\pi r^2$ . Experimentally, controlling the density is difficult. We find it easier to control the radius of the central column, thereby manipulating its strength (however, this method introduces the possibility of finite vortex size issues). As an

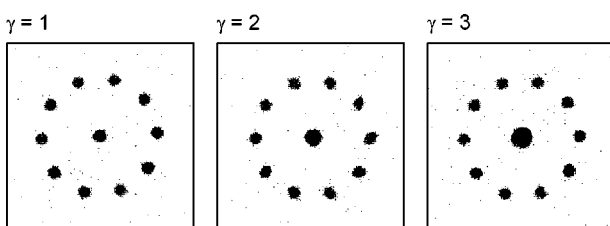


FIG. 5.  $N=10+1$  initial states, demonstrating how we manipulate the central vortex's strength by controlling its size.

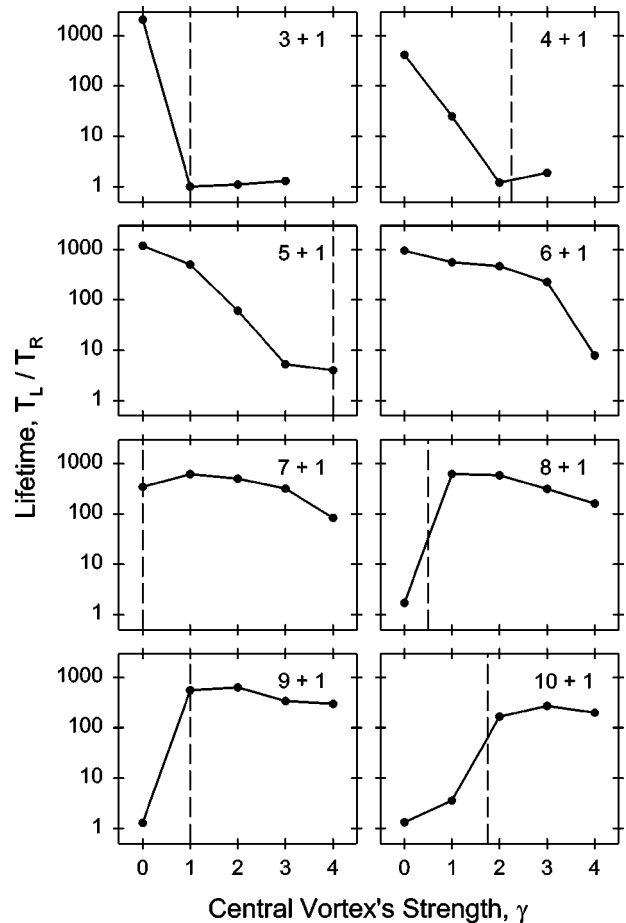


FIG. 6. Lifetime vs the central vortex's strength, for  $N$  vortices arranged in a ring with a central vortex. For  $N=3+1$  to  $5+1$ , the upper stability limit is indicated by the dashed line (the lower limit is off-scale). For  $N=7+1$  to  $10+1$ , the lower stability limit is indicated (the upper limit is off-scale). Both limits are off-scale for  $N=6+1$ .

example, Fig. 5 shows initial states for  $N=10+1$  vortices.  $\gamma$  is defined as the central vortex's strength normalized by a ring vortex's strength. For our experimental parameters, we find that this technique works well for  $0 \leq \gamma \leq 4$ . For  $\gamma > 4$ , the stronger central electron column shears the ring columns during the injection.

Figure 6 summarizes the experimental lifetimes for  $N=3+1$  to  $10+1$ , demonstrating general but not complete agreement with the predicted stability limits.

(1) For  $N=3+1$  to  $5+1$ , we are able to probe  $\gamma$ 's upper stability limit, but not its lower limit ( $\gamma_{\text{lower}} < 0$ ). The agreement is excellent for  $N=3+1$  and  $4+1$ , but poor for  $5$

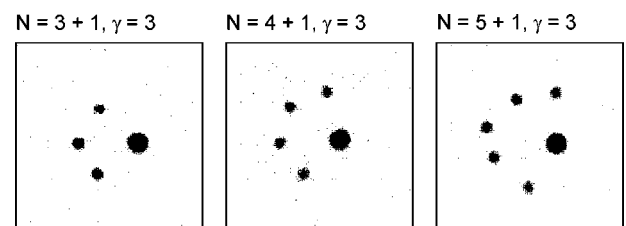


FIG. 7. A selection of stable patterns that emerge when probing the upper stability limit of  $\gamma$ . Each lives for another  $500 T_R$ .

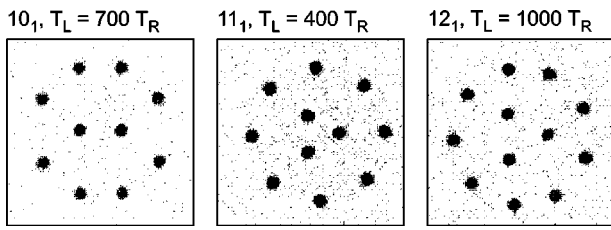


FIG. 8. The initial states and lifetimes for three more complicated vortex patterns.

+1. Figure 7 shows a selection of stable patterns that emerge from initially unstable patterns (because  $\gamma \neq 1$ , these patterns are not in The Catalog). Since these patterns emerge very early during the evolution ( $\approx 10 T_R$ ), the evolutions and subsequent recrystallizations could be influenced by the injected background electron density (thereby possibly accounting for the poor behavior of  $N = 5 + 1$ ). The emerged patterns are all long lived ( $T_L \approx 500 T_R$ ) and therefore very stable.

(2) For  $N = 6 + 1$ , the theoretical stability limits are no longer accessible with the current setup ( $-0.25 \leq \gamma \leq 6.25$ ). Agreement with the upper limit is poor and patterns similar to those in Fig. 7 emerge. Again, injected background electron density is suspect.

(3) For  $N = 7 + 1$  to  $10 + 1$ , we are able to probe  $\gamma$ 's lower stability limit, but not its upper ( $\gamma_{\text{upper}} \geq 9$ ). Here, the agreement with theory is excellent.

V. MORE COMPLICATED PATTERNS

2-D vortex patterns are not constrained to a ring. Figures 8 and 9 show more complicated patterns from The Catalog and their lifetimes; all are stable ( $T_L > 100 T_R$ ), as predicted.

Figure 9 shows a special class of patterns composed of triangular numbers of vortices,  $N = 1 + 6(1 + 2 + 3 + \dots)$ . To inject these patterns, we used smaller radii electron columns, 0.020 cm. The distance between adjacent rings of columns is 0.20 cm, so that the  $N = 61$  pattern has an outer radius of 0.80 cm, normalized by the outer boundary radius to 0.40. When the outer radius is greater than approximately 0.5, we find that patterns are destabilized by the boundary.

Figure 10 shows a pattern for  $N = 6$  that is not in The Catalog. This pattern emerged from a maximum entropy theory developed by Jin and Dubin to predict the evolution of stable vortex patterns from the turbulent decay of an electron system.<sup>14</sup> This research inspired Coppa to analytically study the stability of two sets of  $N$  vortices with strengths  $\gamma_1$  and  $\gamma_2$  arranged in two rings with radii  $r_1$  and  $r_2$  in a

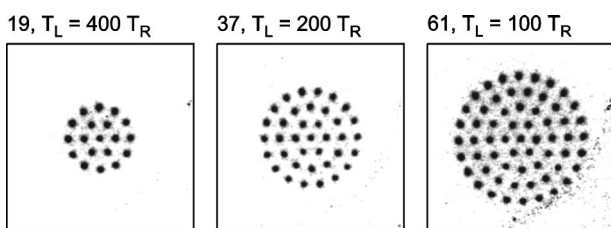


FIG. 9. The initial states and lifetimes for patterns composed of triangular numbers of vortices.

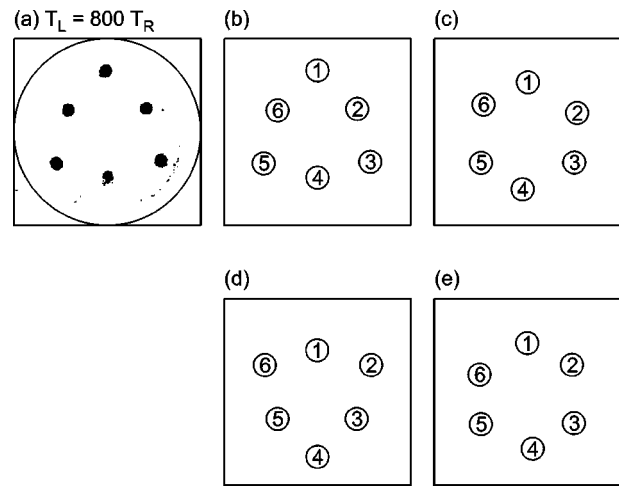


FIG. 10. (a) An  $N = 6$  pattern that requires the boundary for stability. A smaller version, farther from the boundary, breathes between the states in the rotating frame shown in (b)–(e).

boundary.<sup>27</sup> If  $\gamma_1 = \gamma_2$  and  $r_1 = 0.66$ , then a stable pattern will have  $r_2 = 0.49$  (from Coppa's formulas), as shown in Fig. 10(a); experimentally, it lives for over 800 bulk rotations. We also experimented with a smaller version:  $r_1 = 0.25$  and  $r_2 = (0.49/0.66)(0.25) = 0.19$ . The initial state in Fig. 10(b) exhibits a curious breathing motion around the stable  $N = 6$  hexagon. The patterns oscillate between near-triangular and near-hexagonal states in the reference frame rotating with the pattern, as shown in Figs. 10(b)–10(e). One breath takes approximately 1.5 bulk rotations and continues for over 1000 bulk rotations.

VI. SUMMARY

Experiments on the stability of  $N$  vortices arranged in a ring, for  $N = 2 - 10$ , demonstrate excellent agreement with theory. For most cases, the stability of  $N$  vortices arranged in a ring with a central vortex, for  $N = 3 + 1$  to  $10 + 1$ , demonstrate good agreement with the predicted stability limits on the central vortex's strength. The stability of more complicated vortex patterns from The Catalog is explored, again with excellent agreement. Moreover, stable vortex patterns sometimes emerge from unstable patterns; when these patterns consist of equal strength vortices, they are in The Catalog. These experiments demonstrate the photocathode's utility for testing 2-D fluid theories in a Malmberg–Penning trap.

ACKNOWLEDGMENTS

We thank L. Zimmerman for her assistance with the patterns of triangular numbers. This work was supported by the Office of Naval Research.

<sup>1</sup>W. T. Kelvin, *Mathematical and Physical Papers* (Cambridge University Press, 1878), Vol. IV, p. 135.  
<sup>2</sup>J. Thomson, *Treatise on Vortex Rings* (Macmillan, London, 1883), p. 94.  
<sup>3</sup>T. Havelock, "The stability of motion of rectilinear vortices in ring formation," *Philos. Mag.* **11**, 617 (1931).  
<sup>4</sup>E. Yarmuck, M. Gordon, and R. Packard, "Observation of stationary vortex arrays in rotating superfluid helium," *Phys. Rev. Lett.* **43**, 214 (1979).

- <sup>5</sup>E. Yarmuck and R. Packard, "Photographic studies of quantized vortex lines," *J. Low Temp. Phys.* **46**, 479 (1982).
- <sup>6</sup>L. Campbell and R. Ziff, "A catalog of two-dimensional vortex patterns," Los Alamos Scientific Laboratory Report No. LA-7384-MS, 1978.
- <sup>7</sup>L. Campbell and R. Ziff, "Vortex patterns and energies in a rotating superfluid," *Phys. Rev. B* **20**, 1886 (1979).
- <sup>8</sup>J. H. Malmberg, C. F. Driscoll, B. Beck, D. L. Eggleston, J. Fajans, K. Fine, X. P. Huang, and A. W. Hyatt, in *Nonneutral Plasma Physics*, edited by C. Roberson and C. Driscoll (American Institute of Physics, New York, 1988), Vol. 175, p. 28.
- <sup>9</sup>*Non-Neutral Plasma Physics II*, edited by J. Fajans and D. H. E. Dubin (American Institute of Physics, New York, 1995), Vol. 331.
- <sup>10</sup>R. H. Levy, "Diocotron instability in a cylindrical geometry," *Phys. Fluids* **8**, 1288 (1965).
- <sup>11</sup>R. J. Briggs, J. D. Daugherty, and R. H. Levy, "Role of Landau damping in crossed-field electron beams and inviscid shear flow," *Phys. Fluids* **13**, 421 (1970).
- <sup>12</sup>C. F. Driscoll and K. S. Fine, "Experiments on vortex dynamics in pure electron plasmas" *Phys. Fluids B* **2**, 1359 (1990).
- <sup>13</sup>K. Fine, A. Cass, W. Flynn, and C. Driscoll, "Relaxation of 2D Turbulence to Vortex Crystals," *Phys. Rev. Lett.* **75**, 3277 (1995).
- <sup>14</sup>D. Jin and D. Dubin, "Regional maximum entropy theory of vortex crystal formation," *Phys. Rev. Lett.* **80**, 4434 (1998).
- <sup>15</sup>D. A. Schecter, D. H. E. Dubin, K. S. Fine, and C. F. Driscoll, "Vortex crystals from 2D Euler flow: Experimentation and simulation," *Phys. Fluids* **11**, 905 (1999).
- <sup>16</sup>D. Durkin, "Experiments on 2D vortex patterns in a Malmberg-Penning trap with a photocathode," Ph.D. thesis, University of California, Berkeley, 1998.
- <sup>17</sup>D. Durkin and J. Fajans, "A photocathode source for studying two-dimensional fluid phenomena with magnetized electron columns," to be published in *Rev. Sci. Instrum.*
- <sup>18</sup>A. J. Peurrung and J. Fajans, "A limitation to the analogy between pure electron plasmas and 2-D inviscid fluids," *Phys. Fluids B* **5**, 4295 (1993).
- <sup>19</sup>B. P. Cluggish and C. F. Driscoll, "Transport and damping from rotational pumping in magnetized electron plasma," *Phys. Rev. Lett.* **74**, 4213 (1995).
- <sup>20</sup>J. Kriesel, "Experiments on viscous and asymmetry-induced transport in magnetized, pure electron plasmas," Ph.D. thesis, University of California, San Diego, 1999.
- <sup>21</sup>D. H. E. Dubin and T. M. O'Neil, "Two-dimensional bounce-averaged collisional particle transport in a single species non-neutral plasma," *Phys. Plasmas* **5**, 1305 (1998).
- <sup>22</sup>D. G. Dritschel, "The stability and energetics of corotating uniform vortices," *J. Fluid Mech.* **157**, 95 (1985).
- <sup>23</sup>T. B. Mitchell and C. F. Driscoll, "Electron vortex orbits and merger," *Phys. Fluids* **8**, 1828 (1996).
- <sup>24</sup>G. Morikawa and E. Swenson, "Interacting motion of rectilinear geostrophic vortices," *Phys. Fluids* **14**, 1058 (1971).
- <sup>25</sup>L. J. Campbell, "Transverse normal modes of finite vortex arrays," *Phys. Rev. A* **24**, 514 (1981).
- <sup>26</sup>I. Lansky and T. O'Neil, "Stability analysis of a two-dimensional vortex pattern," *Phys. Rev. E* **55**, 7010 (1997).
- <sup>27</sup>G. G. M. Coppa, "Equilibrium and stability for two-ring patterns of vortices in a Penning trap," PT DE 504/IN, Politecnico di Torino, Torino (Italy), 1999.